

DIJET SIGNALS OF THE LITTLE HIGGS MODEL WITH T-PARITY

Debajyoti Choudhury,^{1,*} Dilip Kumar Ghosh,^{2,†} and Santosh Kumar Rai^{3,‡}

¹*Department of Physics and Astrophysics,
University of Delhi, Delhi 110007, India.*

²*Department of Theoretical Physics, Indian Association for the Cultivation of Science,
2A & 2B Raja S.C. Mullick Road, Kolkata 700 032, India.*

³*Department of Physics and Oklahoma Center for High Energy Physics,
Oklahoma State University, Stillwater, OK 74078-3072, USA*

The Littlest Higgs model with T -parity (LHT), apart from offering a viable solution to the naturalness problem of the Standard Model, also predicts a set of new fermions as well as a candidate for dark matter. We explore the possibility of discovering the heavy T -odd quark Q_H at the LHC in a final state comprising two hard jets with a large missing transverse momentum. Also discussed is the role of heavy flavor tagging.

PACS numbers: 12.60.-i, 14.65.Jk, 13.87.Ce

*Electronic address: debchou@physics.du.ac.in

†Electronic address: tpdkg@iacs.res.in

‡Electronic address: santosh.raai@okstate.edu

I. INTRODUCTION

Little Higgs models [1] offer an intriguing resolution of the fine-tuning problem associated with electroweak symmetry breaking. Incorporating the standard model (SM) Higgs as a pseudo-Goldstone boson of some global symmetry which is spontaneously broken at a scale $\Lambda(\equiv 4\pi f) \sim 10$ TeV, the low energy effective theory is described by a non-linear sigma model. With the introduction of new gauge bosons and partners of the top quark with masses of the order of f , the quadratically divergent contributions to the Higgs mass are exactly cancelled at one loop level, thereby ameliorating the fine-tuning problem.

However, constraints from precision electroweak measurements imply that the scale f needs to be above ~ 5 TeV [2]. For such a large value of f , one faces the re-introduction of a fine tuning between the cutoff scale ($\sim 4\pi f$) for the model and the weak scale. To circumvent this serious problem of the original Little Higgs model, a new discrete symmetry, called T -parity (and analogous to the R parity in the minimal supersymmetric standard model), was introduced. The Littlest Higgs Model with T -parity (LHT) [3–6] provides a fully realistic and consistent model which satisfies the electroweak precision data. All SM fields are T -even under this new symmetry, while the new heavy partners are T -odd, and can only be produced in pairs. Moreover, even after electroweak symmetry breaking, mixing between the SM gauge bosons and their T -odd counterparts is prohibited, thereby removing any tree level new physics contribution to the electroweak precision observables. Consequently, all new physics corrections now appear only at the one loop level or higher, and, hence, are naturally small. As a result, the EW precision data concede a relatively low value of the new particle mass scale $f \sim 500$ GeV [5], thereby allowing copious production of different T -odd heavy partners of the SM particles at the LHC and future e^+e^- linear collider (ILC) [4, 7–13].

A further interesting feature of T -parity is the prediction of a colorless neutral weakly interacting stable T -odd particle (LTP) A_H , the heavy partner of the hypercharge gauge boson; known as the *heavy photon*, it is a good candidate for cold dark matter [14].

In this paper, we revisit the LHC signatures of T -odd heavy quark pair production within this model. As with a host of other models for new physics beyond the SM, signatures in a hadronic environment are often the easiest to tag on to when cascade decays (hopefully, with

isolated hard leptons) are considered [7–9, 11, 12, 15]. This, indeed, happens in the LHT models for a significant range of parameters. However, for a large range, cascade chains do not occur and the T -odd quarks decay promptly into the A_H and a SM quark. The consequent final state, namely a dijet pair alongwith missing transverse energy, is relatively more difficult to analyse and this had led to search strategies ignoring this important part of the parameter space. In the case of the third generation (down-type) heavy T -odd quark pair production, the final state jets, when tagged, give rise to $2b$ -jet final state, while untagged jets contribute to the dijet cross-section from the pair production of first two generation T -odd heavy quarks. Performing a detailed estimation of the observability of this signal, and taking into account all relevant SM backgrounds, we delineate the additional part of the LHT parameter space that is amenable to discovery at the LHC.

The rest of the paper is organized as follows. In Section II, we briefly discuss the main features of the model. In Section III, we discuss pair production of T -odd heavy quarks and their two body decay into standard model quarks and the LTP, A_H . In Section IV, after discussing signal and background events, we estimate the detectability of the LHT signal in the dijet plus missing energy channel at the LHC. Finally, our conclusions are given in Section V.

II. THE MODEL

Rather than attempting a detailed study of the Littlest Higgs model with T -parity (see, for example, Refs.[3–5]), we concentrate on the issues directly relevant to us. Considering a non-linear sigma model with a $SU(5)$ global symmetry, let us gauge the subgroup $[SU(2) \times U(1)]_1 \times [SU(2) \times U(1)]_2$. A discrete symmetry (T -parity) exchanges the two $[SU(2) \times U(1)]$ units, thereby restricting the matter content as well as the gauge couplings. The global $SU(5)$ is broken down to $SO(5)$ at some high scale f , leading to 14 massless Nambu-Goldstone (NG) bosons [1]. Simultaneously, the gauged symmetry is broken down to the diagonal subgroup $SU(2)_L \times U(1)_Y$ to be identified with the SM gauge group. Of the 14 NG bosons, four are manifested as the longitudinal modes of the heavy gauge bosons. The remaining ten decompose into a T -even $SU(2)$ doublet h , identified with the SM Higgs field, and a

complex T -odd $SU(2)$ triplet Φ , which obtains a mass $M_\Phi = \sqrt{2}M_h f/v_{\text{SM}}$ at one loop, with M_h being the SM Higgs mass.

Not being singlets under the SM gauge group, the T -odd acquire further contributions to their masses from electroweak symmetry breaking, and we have

$$\begin{aligned} M_{A_H} &\simeq \frac{g'f}{\sqrt{5}} \left[1 - \frac{5v_{\text{SM}}^2}{8f^2} + \dots \right] , \\ M_{Z_H} &\simeq M_{W_H} = gf \left[1 - \frac{v_{\text{SM}}^2}{8f^2} + \dots \right] . \end{aligned} \quad (1)$$

Here, $v_{\text{SM}} \simeq 246$ GeV is the electroweak symmetry breaking scale. Since $g' < g$, A_H is substantially lighter than other two T -odd heavy gauge bosons W_H and Z_H .

Consistent implementation of T -parity in the fermion sector requires that each SM fermion doublet must be replaced by a pair of fields $F_i (i = 1, 2)$ [3–5], where each F_i is a doublet under $SU(2)_i$ and singlet under the other. Under T -parity, $F_1 \leftrightarrow F_2$ and the T -even combination of F_i is identified with the SM fermion doublet. The other (T -odd) combination is its heavy partner (F_H). To generate mass terms for the latter, one requires an extra set of T -odd $SU(2)$ singlet fermions in the theory [3–5]. Considering an universal and flavour diagonal Yukawa coupling κ for U_H and D_H (the T -odd heavy partners of the SM quarks (u, c) and (d, s) respectively), we have

$$M_{D_H} \simeq \sqrt{2} \kappa f , \quad M_{U_H} \simeq \sqrt{2} \kappa f \left(1 - \frac{v_{\text{SM}}^2}{8f^2} \right) . \quad (2)$$

Since $f \gtrsim 500$ GeV, it is evident from eq.(2) that the up- and down-type T -odd heavy partners have nearly equal masses. In summary, the complete spectrum of the LHT model with T -parity relevant for our analysis will only depend on two free parameters: the new physics scale f and the flavour independent Yukawa coupling κ .

III. PRODUCTION AND DECAY OF THE 1st AND 2nd GENERATION T -ODD HEAVY QUARK

Given the model described in the preceding section, we may calculate the production rates of T -odd quarks at the LHC. The latter can be copiously pair produced ($Q_H \bar{Q}_H$) as long as their masses are not too large. The LHC being primarily a gluon machine,

the pure QCD process naturally dominates, and the calculation thereof is identical to that for any heavy quark [16]. However, even the electroweak amplitudes do have substantial contributions, especially for like-sign Q_H production [12]. To discuss these, we need to know the electroweak couplings of the T -odd quarks.

The $Q_H q^{(\prime)} V_H$ couplings (where V_H is one of W_H , Z_H and A_H) depend on f . The couplings $U_H - d - W_H$ and $D_H - u - W_H$ are of equal strength owing to $SU(2)$ invariance of the Lagrangian, viz.

$$g_{U_H d W_H} = g_{D_H u W_H} = g/\sqrt{2}. \quad (3)$$

On the other hand, the couplings to the Z_H and A_H have a crucial dependence on isospin (T_3), namely

$$g_{f_H f Z_H} = g c_H T_{3f} + g' s_H Y', \quad g_{f_H f A_H} = -g s_H T_{3f} + g' c_H Y', \quad (4)$$

where $Y' = -1/10$ and θ_H is the Weinberg angle in the heavy sector, viz.

$$s_H \equiv \sin \theta_H \simeq \frac{5 g g'}{5 g^2 - g'^2} \frac{v_{\text{SM}}^2}{4 f^2}, \quad c_H \equiv \cos \theta_H. \quad (5)$$

Eq.(4) immediately opens up the possibility for a cancellation in $g_{D_H d A_H}$, especially for smaller f values.

Before discussing the production, let us comment about its aftermath, namely the decays. Once these heavy T -odd quarks are produced, they will promptly decay into (T -even) SM quarks and T -odd heavy gauge bosons (W_H^\pm, Z_H, A_H). As the W_H^\pm/Z_H are themselves unstable, decays into these channels would lead to cascades and the corresponding signatures have been well-studied in the literature, albeit for differing regions in the parameter space. Instead, we concentrate on the decays $Q_H \rightarrow q + A_H$. As a comparison of eq.(2) with eqs.(1) shows, the U_H and D_H are heavier than W_H/Z_H only if κ is not too small¹. Also important are the parameter-dependences of the $f_H f' V_H$ couplings, in particular the suppression of $\Gamma(D_H \rightarrow d + A_H)$ for small f .

¹ Note that a very small κ is disallowed as this would render Q_H to be stable and, hence, lead to a colored and charged dark matter candidate! On the other hand, in the fine-tuned case of Q_H being only marginally heavier than the A_H , it would be quasi-stable on detector scales, leading to the formation of states analogous to R -hadrons [17]. We shall not consider such finely-tuned scenarios.

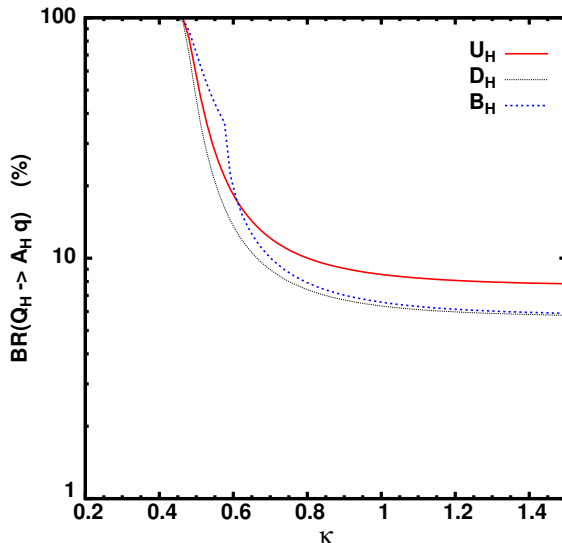


FIG. 1: Variation of the branching ratio of heavy quarks (Q_H) into $q + A_H$ in the LHT model with the parameter κ for a fixed value of the scale parameter $f = 1000$ GeV.

In Fig. 1, we display the two-body decay branching probability for the T-odd quarks U_H, D_H and B_H . For $\kappa \lesssim 0.45$, the two-body decay mode into A_H is the only kinematically allowed one². For $\kappa \gtrsim 0.45$, though, the other modes are accessible, and the two-body branching into A_H drops very fast, essentially on account of the larger coupling to the W_H . For a sufficiently large κ , the kinematical suppression is rendered irrelevant and the branching fraction is determined only in terms of the coupling constants. The branching for the B_H shows a small kink at $\kappa \sim 0.6$ as the tW_H decay mode becomes available only at this juncture³.

We now turn to the production of Q_H pairs. As the heavy quarks corresponding to the first two generations are nearly degenerate, and lead to very similar final state configurations, we sum over all four flavours. Understandably, the pure-QCD processes $gg \rightarrow Q_{iH}\bar{Q}_{iH}$ and $q_j\bar{q}_j \rightarrow Q_{iH}\bar{Q}_{iH}$ tend to dominate and was considered in Ref [18]. The ordinary electroweak contributions to the $q\bar{q}$ -initiated process is only $\mathcal{O}(\alpha_{\text{wk}}^2)$. As for the V_H mediated contributions, these too are only $\mathcal{O}(\alpha_{\text{wk}}^2)$ unless $i = j$, whence it can be $\mathcal{O}(\alpha_s \alpha_{\text{wk}})$. Note, though, that $\kappa \lesssim 0.45$ means that the W_H/Z_H are at least as massive as the Q_H and this implies

² For T_H , depending on the value of f , it could even be that $T_H \rightarrow A_H + b + W^+$ is the only one allowed.

³ Clearly, the exact location of this kink depends on the value of f .

additional suppression; and while the A_H -diagram is not suppressed kinematically, it is virtually irrelevant for D_H production (owing to the smaller cross-sections). Thus, in effect, most of the electroweak contributions are expected to be rather subdominant. However, we must note that for large values of f , the partons are required to carry a bigger momentum fraction x of the proton. This, in turn, renders the valence quark induced subprocesses (mediated by V_H) to be comparable to or even dominate the gluon initiated subprocesses. Thus, processes such as $u q_j \rightarrow U_H Q_{jH}$ (where $j=1,2$) cannot be neglected anymore as, for example, was done in Ref [18]. We, on the other hand, include all processes (and all amplitudes) that lead to the production of a pair of heavy quarks ($Q_{iH} Q_{jH} (\bar{Q}_{jH})$), irrespective of the flavour composition.

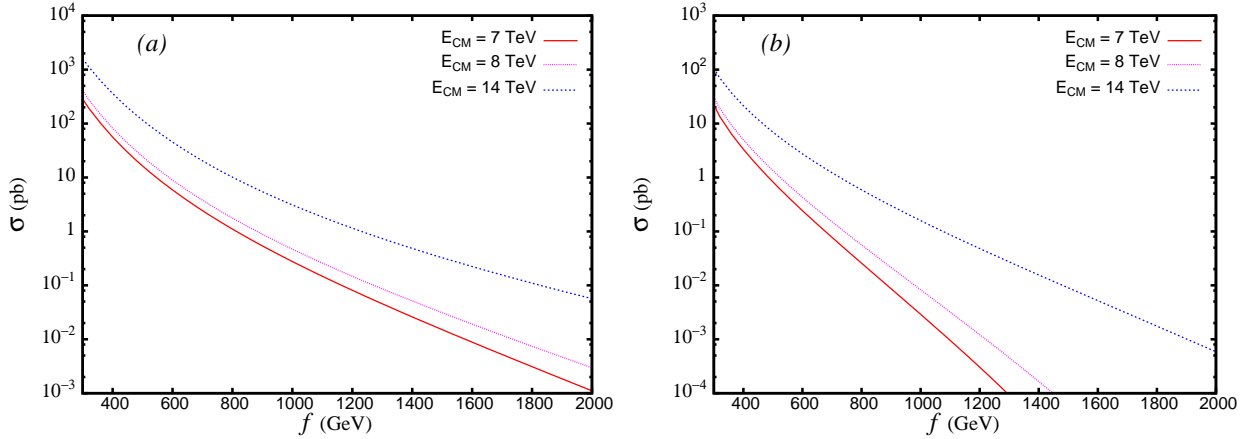


FIG. 2: The variation of the leading order T -odd quark pair ($Q_H \bar{Q}_H + Q_H Q_H + \bar{Q}_H \bar{Q}_H$) production with the scale f for (a) $\kappa = 0.45$ and (b) $\kappa = 1.0$ for the LHC running at $\sqrt{s} = 7, 8, 14$ TeV

In our numerical analysis, we use the CTEQ6L1 parton distribution functions [19]. In the absence of higher order calculations, we consider only the leading-order processes. For the pure QCD processes, the K -factor, parametrizing the higher-order contributions to the production cross section, could, in principle, be estimated from analogous calculations for the top-quark [20] and is somewhat larger than unity. For the electroweak processes, though, such calculations are not available. Given this, we adopt the *conservative* approach of both neglecting the K -factor as well as choosing a moderate factorisation scale, viz. $Q = \sqrt{\hat{s}}/2$. In Fig. 2, we display the production rate of the T -odd quark as a function of the scale f for two

values of the parameter κ namely $\kappa = 0.45$ and 1.0 for a few choices of the LHC operating energy. While the pure QCD amplitude depends only on the mass of the heavy quark, and thus on the product κf alone, the electroweak amplitudes have additional dependence on f (owing, *e.g.*, to the t -channel exchange of $W_H/Z_H/A_H$ *etc.*). In addition, both the branching fractions as well as the decay distributions have further dependence on the scale f .

In particular, we choose four representative values for the scale f (while keeping fixed $\kappa = 0.45$) for all the simulations. In Table I, we list the relevant parts of the corresponding mass spectra as also the total production cross section for pairs of Q_H (limiting ourselves to the partners of the first two generations). These, then, serve as our benchmark points

| f (GeV) | $M_{Q_H}^{(U,D)}$ (GeV) | M_{A_H} (GeV) | $\sigma(\sum Q_H - pair)$ (fb) | | |
|-----------|-------------------------|-----------------|--------------------------------|-----------------------|--------------------|
| | | | 7 TeV | 8 TeV | 14 TeV |
| 750 | (470.9, 477.3) | 111.9 | 1.62×10^3 | 2.56×10^3 | 1.42×10^4 |
| 1000 | (631.6, 636.4) | 153.9 | 2.76×10^2 | 4.69×10^2 | 3.10×10^3 |
| 1500 | (951.4, 954.9) | 235.8 | 1.51×10^1 | 3.12×10^1 | 3.26×10^2 |
| 2500 | (1589, 1591) | 397.3 | 8.17×10^{-2} | 3.09×10^{-1} | 1.25×10^1 |

TABLE I: *The mass spectrum for the T-odd quarks of the first two generations and the lightest stable T-odd particle for four different choices of the scale f with $\kappa = 0.45$. We also list the total pair production cross section for the T-odd heavy quarks at LHC with center-of-mass energies of 7 TeV, 8 TeV and 14 TeV respectively.*

(except for $f = 2.5$ TeV at $\sqrt{s} = 7$ TeV in view of the smallness of the cross section).

IV. RESULTS AND ANALYSIS

A. Dijet signal

We now focus on the dijet plus missing energy channel in the LHT model and compare it against the SM expectations. A hadronic machine such as the LHC is associated with large rates for QCD processes and inclusive dijet production is the dominant mode in SM, with

cross-sections of the order of a few *millibarns*. Thus, it poses the most serious background for any new physics signal in this particular channel. While new physics signals with strong dynamics and resonances in the dijet invariant mass which are expected to stand out over the QCD background have been studied in the literature [21–28], no such resonance is expected in the LHT model. Instead, dijets are produced in association with the lightest massive stable particles, which give rise to a significant amount of missing transverse momenta. This renders difficult the observation of such signals over the QCD background. Consequently, most search strategies have concentrated on cascade decay modes instead. However, as we have already argued in the preceding section, for $\kappa \lesssim 0.45$, the cascade decay modes disappear and the only final state available to us is that comprising two hard jets accompanied by missing transverse momentum.

To be specific, we shall choose $\kappa = 0.45$, unless otherwise stated. For a given f , this implies the most massive Q_H (and, hence, the smallest production cross sections) consistent with a dominant decay mode into a SM quark and the LTP. Understandably, the signal is completely overwhelmed by the large QCD background. Also to be included in the background are other multijet sub-processes, accruing dominantly from resonant processes in the SM, such as those involving the weak gauge bosons (W^\pm, Z).

The SM backgrounds, irrespective of their origin (viz, QCD, $t\bar{t}$ production, W^\pm/Z with or without jets) were generated with PYTHIA [29], thereby allowing us to include the effects of ISR/FSR, showering and hadronization. Those backgrounds (such as (di-)boson production with hard jets) that cannot be computed directly thus, were generated with ALPGEN[30]. These, though, turned out to be of little consequence. The signal events, on the other hand, were generated with CalcHEP [31] and then interfaced with PYTHIA.

The jets were constructed using the inbuilt toy calorimeter subroutine PYCELL which is a jet clustering algorithm and is used to get the final state jets for the analysis. We define two jets to be separately distinguishable, if they satisfy

$$\Delta R_{jj} = \sqrt{(\Delta\eta)^2 + (\Delta\phi)^2} > 0.7, \quad (6)$$

where $\Delta\eta$ and $\Delta\phi$ are their separations in rapidity and azimuthal plane respectively. Any pair of jets that does not satisfy this is merged. We require that the final state have *exactly*

two jets satisfying

$$\begin{aligned} p_T^{j_i} &> 100 \text{ GeV}; \quad (i = 1, 2) \\ |\eta_j| &< 2.5 \end{aligned} \tag{7}$$

where the jets (j_1 & j_2) are ordered according to their transverse momenta ($p_T^{j_1} > p_T^{j_2}$) and η_j represents their individual rapidities. In other words, we veto events containing a third jet satisfying eq.(7). We also veto events with an isolated lepton (*i.e.*, satisfying $\Delta R_{j\ell} > 0.4$ for each jet) with a $p_T > 10$ GeV and falling within the detector coverage ($|\eta_\ell| < 2.5$). To improve the signal to background ratio, we also impose

$$\sum p_T^{j_1, j_2} \equiv p_T^{j_1} + p_T^{j_2} > 500 \text{ GeV}. \tag{8}$$

For future reference, we designate the combination of cuts in eqs.(7 & 8) by \mathcal{C}_1 .

A final state such as ours affords very few kinematical variables that could be exploited to improve the signal to noise ratio. Indeed, the only other obvious independent cut would be one on the missing transverse momentum \cancel{p}_T . However, rather than imposing a flat requirement on \cancel{p}_T , we instead consider a related variable α_T advocated, in an entirely different context, by Ref.[32]. Expressible as the ratio of the transverse momenta of the second leading jet and the invariant mass of the dijet pair, it is given by

$$\alpha_T \equiv \frac{p_T^{j_2}}{M_{jj}}. \tag{9}$$

It is easy to see that, for an exclusive dijet event (*i.e.*, one with no other hard visible object and/or substantial \cancel{E}_T), $p_T^{j_2} = p_T^{j_1}$ and $2\alpha_T = |\sin\theta|$, with θ being the scattering angle in the parton center of mass frame. Thus, if \cancel{E}_T is to originate from mismeasurements of the jet energies, then the corresponding ratio satisfies $\alpha_T \lesssim 0.5$. Even with the emission of further jets, the situation is not expected to vary radically as long as the extra jets are not too hard. Indeed, as ref.[32] has argued, the entire QCD background trails off beyond $\alpha_T \gtrsim 0.5$. The configuration would be substantially different, though, if the dijet pair recoils against a massive particle (say a Z) or any other source of a substantial \cancel{p}_T . This prompts us to invoke the final selection cut (called \mathcal{C}_2) namely

$$\alpha_T \geq 0.51. \tag{10}$$

The dominant SM background is that due to the $2 \rightarrow 2$ hard QCD sub-processes. Although the hard process, *per se*, is not associated with any missing transverse momentum,

some amount of \cancel{p}_T can arise either from the jets fragmenting into neutrinos or simply from a mismeasurement of the jet energy. To parametrize the latter, we effect a Gaussian smearing of the jet energy with a resolution given by

$$\frac{\Delta E}{E} = \frac{0.8}{\sqrt{E} \text{ (GeV)}}.$$

Note that this is substantially worse than, say, the CMS resolution in the barrel region (to which we limit our detection) [33], and, thus, represents a *deliberately conservative choice*. Also included are the other backgrounds, for example, those emanating from W +jets, Z +jets and $t\bar{t}$ production.

| Cut flow | Signal (fb) | | | SM background (fb) | | | |
|---------------------------------|-------------|-------|------|-------------------------|------------|------------|------------|
| | f (TeV) | | | | | | |
| | 0.75 | 1.0 | 1.5 | QCD | $t\bar{t}$ | $W + jets$ | $Z + jets$ |
| \mathcal{C}_1 | 84.80 | 36.10 | 5.37 | $\sim 1.62 \times 10^5$ | 92.50 | 710.03 | 272.02 |
| $\mathcal{C}_1 + \mathcal{C}_2$ | 2.16 | 2.79 | 1.05 | $\simeq 13.01$ | 0.05 | 0.21 | 0.38 |

TABLE II: *The leading-order cross sections for the $2j + \cancel{E}_T$ final state at LHC with $\sqrt{s} = 7$ TeV for three benchmark points of the LHT model with a fixed $\kappa = 0.45$. We also list the rates for the dominant SM backgrounds.*

The entries in the first row of Tables II & III show the cross sections for the benchmark points on imposition of the aforementioned selection cuts \mathcal{C}_1 (but not \mathcal{C}_2). The suppression of the signal strength due to the cuts is clearly discernible. As a comparison with Table I shows, this suppression is progressively less severe as the scale f increases. This is easy to appreciate as a larger value of f implies not only larger masses for the Q_H , but also larger split between m_{Q_H} and m_{A_H} . This, in turn, leads to harder jets from the decay of the Q_H , thereby satisfying eq.(8) with relative ease.

What is more important is that, on imposition of the cuts \mathcal{C}_1 alone, the QCD background is ~ 162 (1140) pb for the LHC operating at $\sqrt{s} = 7$ (14) TeV. This is orders of magnitude larger than the signal cross sections of Tables II & III. Even the electroweak backgrounds are larger than the signal. This necessitates the use of additional cuts and, to this end, we must

| Cut flow | Signal (fb) | | | | SM background (fb) | | | |
|---------------------------------|--------------------|--------|--------|------|-------------------------|--------------------|--------------------|--------------------|
| | $f(\text{TeV})$ | | | | | | | |
| | 0.75 | 1.0 | 1.5 | 2.5 | QCD | $t\bar{t}$ | $W + jets$ | $Z + jets$ |
| \mathcal{C}_1 | 1.01×10^3 | 490.03 | 122.04 | 7.09 | $\sim 1.14 \times 10^6$ | 1.23×10^3 | 4.52×10^3 | 1.84×10^3 |
| $\mathcal{C}_1 + \mathcal{C}_2$ | 25.33 | 31.02 | 18.12 | 1.40 | $\simeq 31.79$ | 1.26 | 5.43 | 4.66 |

TABLE III: *As in Table.II, but for $\sqrt{s} = 14 \text{ TeV}$ instead.*

examine the phase space distributions. We present, in Fig.3, the normalized distributions, for both signal and background, in various kinematical variables⁴. As Fig.3(a) shows, the missing E_T distribution for the background is much softer than that for the signal. This is not unexpected as far as the QCD background is concerned, for there the missing E_T arises largely on account of mismeasurement. There is, of course, some contribution from (semi-)leptonic decays of hadrons within a jet, but these are subdominant. The other irreducible SM contribution to this background arises from inclusive Z production followed by $Z \rightarrow \nu_i \bar{\nu}_i$; the corresponding \cancel{p}_T is nothing but the transverse momentum of the Z itself and, hence, is not large. Similar is the story for inclusive W -production, followed by the leptonic W -decays wherein the charged lepton is not registered by the detector.

The missing E_T in the signal events, on the other hand, arises from the decay $Q_H \rightarrow q + A_H$, with the invisible A_H , carrying, in the rest frame of the Q_H , a momentum of $(M_{Q_H}^2 - M_{A_H}^2)/(2 M_{Q_H})$. For the spectrum of Table I this quantity, clearly, is sizable. Understandably, a significant component of the transverse momenta of the two A_H 's may cancel, leading to a smaller discernible \cancel{p}_T . Even then, the spectrum would tend to be hard, typically peaking at nearly $\cancel{p}_T \sim M_{Q_H}/2$.

The invariant mass distribution—Fig.3(b)—although being somewhat different for the signal (as compared to the background constituents), can hardly be used efficiently to improve the signal to noise ratio. Jet separation, on the other hand, is a very useful variable. As Fig.3(c) shows, for the bulk of the background, the two jets are back to back. While this is readily understandable for the QCD component, to appreciate the situation for the

⁴ Although we present here the results for $\sqrt{s} = 14 \text{ TeV}$, those for $\sqrt{s} = 7 \text{ TeV}$ are qualitatively similar.

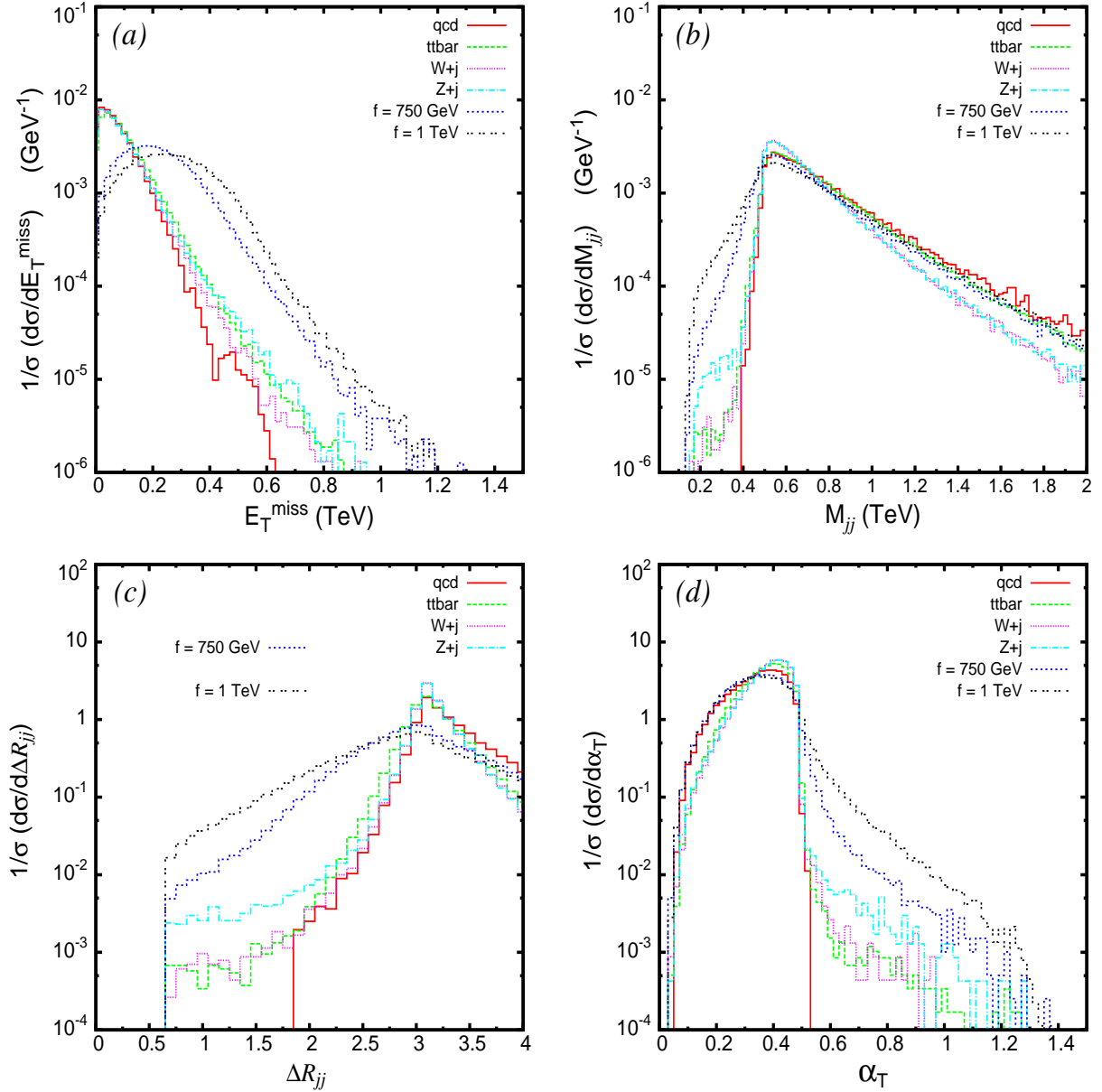


FIG. 3: Normalized differential cross sections, at the LHC ($\sqrt{s} = 14$ TeV), for the signal (2 values of the scale f) and various SM background processes in (a) missing transverse energy, (b) the invariant mass of the two leading jets, ΔR_{jj} between the final state jets, (c) the cone angle between the same, and (d) the variable α_T (see eq.9).

rest of the SM contribution, note that this is but a restatement of the fact that these are characterised by $\not{p}_T/p_T^{j2} \ll 1$. The signal events, on the other hand have a sizable value for this ratio. Indeed, the distributions are correlated and imposing a strong criterion on one

would obviate doing so for the other.

However, instead of imposing cuts on \not{p}_T or ΔR_{jj} , we rather consider the variable α_T . As discussed earlier, this has the advantage of correlating \not{p}_T with the energy scale of the event. As promised and as demonstrated by Fig.3(d), the QCD background falls very sharply for $\alpha_T > 0.5$. While the rates of fall for the other background components are not as severe, the slopes are steep enough for this variable to be considered a good signal to noise discriminator. This conclusion is aided by the fact that the non-QCD backgrounds were subdominant to start with. The signal too peaks at $\alpha_T \lesssim 0.5$. However, the fall beyond $\alpha_T = 0.5$ is much slower indeed. For both the non-QCD background and signal, this extension beyond $\alpha_T = 0.5$ owes its origin to the magnitude of \not{p}_T/p_T^2 .

It might seem at first sight that ΔR_{jj} would do the job as well as α_T . As Fig.3(c) shows, and as we have already discussed, the jet pair is much better separated when it comes to the background (as compared to the signal). However, note that the steepness of the ΔR_{jj}^{SM} distribution is not as pronounced as that of the α_T distribution. Consequently, the improvement in the signal to background ratio is much better when we choose to impose the cut on α_T . This is not surprising because, contrary to simple kinematical variables such as the p_T of an individual jet, \not{p}_T or ΔR_{jj} , the variable α_T is a correlated measure of hardness of the event and the angular separations. This is what has prompted us to choose cut \mathcal{C}_2 in preference to any others.

As Table III shows, the huge background can be effectively eliminated altogether by rejecting all events with $\alpha_T \leq 0.51$. Whereas the majority of the signal events are rejected as well, the signal-to-background ratio improves dramatically. It is interesting to note that the signal efficiency of this α_T cut improves with the increase in the value of the LHT scale f , although the Q_H pair production cross section decreases. This feature is easy to understand. Higher values of f correspond to a heavier LTP and T-odd quarks, which leads to larger imbalance in energy because of heavier LTP which in turn causes a wider spread in the α_T distribution (see Fig. 3 (d)) for $f = 1$ TeV when compared to $f = 750$ GeV. As a result of this, one expects that the α_T cut is less severe for higher values of f leading to better signal significance. Thus, we expect that even though the pair production cross section for T-odd quarks may decrease for large f , the kinematic selection that is most effective in suppressing

the SM background also makes the signal significance better for large values of f . We must, however, note that eventually the small production cross section for very large values of f will take over and make the signal too small to be significant.

The corresponding distributions—for both the signal and background—look very similar for LHC operating at $\sqrt{s} = 7$ TeV, although the event rates are much smaller. Consequently, the α_T cut would work as well for that case. Based on the preceding analysis, a quick and naive estimate of the LHC sensitivity can be made by simply observing the strength of the signal and background events shown in Tables II & III. For the LHC at $\sqrt{s} = 7$ TeV and with the current integrated luminosity $\mathcal{L} \sim 5 \text{ fb}^{-1}$ the sensitivity ($N_s/\sqrt{N_s + N_b}$) is less than 2σ for all the three benchmark points.

It has been now announced that the LHC will run at $\sqrt{s} = 8$ TeV during 2012 and is also expected to deliver a luminosity of 15fb^{-1} for both CMS and ATLAS. Consequently, the total heavy T -odd quark pair production cross-section would increase by a factor varying between 1.16 - 2 for the LHT scale $f = 0.75 - 1.5\text{TeV}$. Even accounting for the increase in the background, the two upgrades, together, would imply that each of ATLAS/CMS would be in a position to report a significant excess by the end of the year if $f \lesssim 1.5$ TeV. A future upgrade of the LHC center of mass energy to $\sqrt{s} = 14$ TeV will be able to probe the LHT model with $f = 0.75 - 1.5$ TeV at 5σ significance in the $2j + \cancel{E}_T$ channel with an integrated luminosity as less as $\mathcal{L} = 3 - 5 \text{ fb}^{-1}$.

B. Heavy flavor-tagged dijet signal

We now specialize to the case where both the jets are b -tagged. Recent analyses at both ATLAS and CMS have shown that a very high efficiency for b -tagging may be obtained [34, 35]. Dependent on the transverse momenta of the b -jets, the efficiencies are as high as 70% for jets with $p_T > 100$ GeV. We work with the same representative points shown in Table I, and where the T -odd B_H decays to the LTP and b -quark with 100% probability for $\kappa < 0.45$, as shown in Fig.1. Since the mass of B_H is degenerate with D_H one expects similar production cross section for them to be pair produced as the D_H states except that the only significant contribution to the cross section comes from the QCD dominated sub-processes. In Fig. 4

we plot the cross section for the process $pp \rightarrow B_H B_H (\bar{B}_H)$ at LHC.

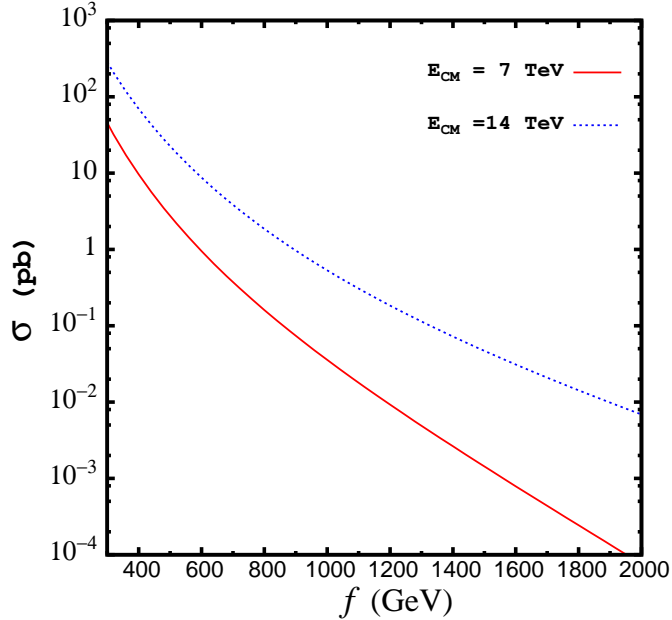


FIG. 4: The variation of the leading order T -odd quark pair $B_H B_H, B_H \bar{B}_H$ production with the scale f for $\kappa = 0.45$ with the LHC running at $\sqrt{s} = 7$ TeV and 14 TeV.

We note that the pair production cross section is about an order of magnitude smaller when compared to the pair production cross section of the first two generation of the T -odd heavy quarks. However, one expects much smaller background for the signal, once the final state jets are tagged as b -jets. The dominant background with very little missing transverse momenta would be the QCD production of $b\bar{b} + X$. In addition the other dominant background comes from the QCD dijet sub-processes for lighter quarks, with the light flavor jets mistagged as b -jets. Though the mistag efficiency for such high p_T light jets is less than 1%, the sheer enormity of the QCD cross section in SM makes it a serious background for the signal. The other major SM backgrounds are due to $W + jets, Z + jets$ and $t\bar{t}$. Note that guided by the previous analysis for the dijet signal, one can easily repeat the same requirements on the phase space to suppress the SM background. For our analysis we demand that both the final state high p_T jets are tagged as b -jets. By doing this we do have a significant suppression for the signal, but demanding such hard b -jets with the kinematic cuts mentioned in Eqs. (8) and (10) effectively suppresses almost all of the SM background,

| Signal (fb) | | | SM background (fb) |
|-----------------------|---------------------|-----------------------|------------------------|
| $f = 750 \text{ GeV}$ | $f = 1 \text{ TeV}$ | $f = 1.5 \text{ TeV}$ | |
| 0.523 (0.045) | 0.767 (0.059) | 0.465 (0.023) | $\simeq 0.242 (0.014)$ |

TABLE IV: *The leading-order cross sections for the $2b - \text{jets} + \cancel{E}_T$ final state at LHC with $\sqrt{s} = 14(7) \text{ TeV}$ for the LHT model with three different choices of the scale f and $\kappa = 0.45$. The cuts are the same as $\mathcal{C}_1 + \mathcal{C}_2$ except for $\Delta R_{bb} > 0.5$*

including that from $W + b\bar{b} + X$ and $t\bar{t}$ ($\lesssim 10^{-3} \text{ fb}$).

For identifying b -jets with the most energetic transverse jets selected we put the condition: a jet is tagged as b -jet if it is associated to a parent b -quark. The identification is made by demanding that the most energetic parton within a cone of radius $\Delta R = 0.5$ around the jet axis is a b quark and also that the opening angle between the b quark and the jet axis lies within 20° . As our b -jets have $p_T > 100 \text{ GeV}$, we assume the average b -tagging efficiency of 50%. For light jets (jets originating in u, d, c, s quarks or in gluons), a fake b -tagging efficiency of 1% is assumed. We consider the same set of kinematics cuts as before except that we put $\Delta R_{bb} > 0.5$. We find that the strong cuts on the b -jet p_T and on the scalar sum along with the α_T cut makes the SM background significantly small albeit comparable to the signal. We list the signal and background cross sections (after all cuts and multiplying with the respective efficiencies) in Table IV. Remembering that what we are looking here is a small subset of the dijet process with reduced efficiencies, it is quite natural to find a much suppressed rate for the $2b$ -jets + \cancel{E}_T signal as compared to the dijet + \cancel{E}_T final state shown in Tables II & III. Understandably, with the present luminosity ($\sim 5\text{fb}^{-1}$), we do not expect any significant excess over the SM prediction for this particular channel. We do not expect any significant enhancement in the $N_s/\sqrt{N_s + N_b}$ even with an increase of center of mass energy of the LHC to 8 TeV with 15fb^{-1} data. However, 3σ signal sensitivity can be obtained for the LHT scale $f = 1 \text{ TeV}$ with an integrated luminosity in excess of 10 fb^{-1} at LHC with $\sqrt{s} = 14 \text{ TeV}$ center of mass energy.

V. CONCLUSIONS

A phenomenological “imperative” in Little Higgs models is the introduction of a T -parity. Apart from predicting a candidate for cold dark matter, this also leads to the presence, in the spectrum, of relatively light T -odd quarks, Q_{iH} which can be copiously pair-produced at the LHC. Canonical search strategies for the same have concentrated on the cascade decay of the Q_{iH} through the T -odd counterparts of the Z and W . For a significantly large fraction of the Littlest Higgs model parameter space, though, such cascades are kinematically forbidden and the Q_{iH} decay directly to a single SM quark and the dark matter candidate A_H .

In this paper, we investigate this very decay, which leads to a final state comprising of a dijet pair alongwith a large missing transverse momentum. To this end, we simulate the production of all possible pairs of $Q_{iH} \bar{Q}_{jH}$ (Q_{jH}), including the electroweak processes. We perform both a parton-level Monte-Carlo, and then generate events using CalcHEP [31] interfaced with PYTHIA [29] thereby allowing us to include the effects of ISR/FSR, showering and hadronization. The jets are constructed using the standard PYTHIA routine PYCELL. The major standard model background for this signal comes from the pure QCD dijet events (with the missing p_T accruing from both the mis-measurement of jet energies as well as the fragmentation into neutrinos), with $W + jets$, $Z + jets$ and $t\bar{t}$ processes also contributing handsomely. All these too are generated using PYTHIA, and cross-checked with ALPGEN [30].

While requiring that there be only two jets with rather stringent demands the scale of the hadronic activity does serve to substantially reduce the background, the latter still overwhelms the signal size. Further demands on the magnitude of missing- E_T does improve the signal-to-background ratio, but it is still not enough (owing largely to the fact that the large hadronic activity itself results in a significant E_T^{miss} accruing from energy mismeasurements). Jet angular separation, on the other hand, plays a crucial role. Although ΔR_{jj} can be used profitably, we find that correlating the jet p_T and their separation through the introduction of the α_T variable (see eq.9) is a far superior alternative. Imposing $\alpha_T > 0.51$ almost entirely eliminates the dominant QCD background, and also reduces the other significantly.

We observe though that, for the LHC at $\sqrt{s} = 7$ TeV and with the current integrated luminosity $\mathcal{L} \sim 5 \text{ fb}^{-1}$, the statistical significance ($N_s/\sqrt{N_s + N_b}$) would be less than 2σ for

all the three benchmark points. However, the recently announced upgrades to a center of mass energy of 8 TeV and an integrated luminosity of 15 fb^{-1} during 2012 raises tantalizing prospects of discovery within the year. Finally, if the LHC attains the center of mass energy of $\sqrt{s} = 14 \text{ TeV}$ it will be able to probe the LHT model with $f = 0.75 - 1.5 \text{ TeV}$ at 5σ significance in the $2j + \cancel{E}_T$ channel with an integrated luminosity as less as $\mathcal{L} = 3 - 5 \text{ fb}^{-1}$.

On the other hand, the pair production of heavy T -odd quark B_H lead to the $2b\text{-jets} + \cancel{E}_T$ signal, where we tag both the b -jets. We find that due to suppressed signal cross-section, probing the LHT model via this particular channel is in fact almost impossible for the LHC operating at $\sqrt{s} = 7 \text{ TeV}$ and the situation remains unchanged even at $\sqrt{s} = 8 \text{ TeV}$. However, at 14 TeV LHC, with an integrated luminosity of $\sim 20 \text{ fb}^{-1}$, we expect to independently probe (with a 3σ significance) the the LHT model in this channel up to a scale $f = 1 \text{ TeV}$.

Before we conclude, it is worth mentioning that the both the ATLAS [36, 37] and CMS [38–40] collaborations have analysed jets plus missing transverse momentum signal in the context of supersymmetric scenarios. However, it should be noted that the difference in spectra between the two cases leads to a marked difference in the cut efficiencies. In other words, the LHT parameter space discussed by us remains unconstrained by the present ATLAS/CMS analyses. Consequently, in our analysis, we have advocated the use of an alternate set of selection cuts, which would serve to increase the sensitivity.

Acknowledgements

D.C. and D.K.G. thank ICTP High Energy Group for their hospitality during a phase of the work. D.K.G. also acknowledges partial support from the Department of Science and Technology, India under the grant SR/S2/HEP-12/2006. S.K.R. would like to thank A. Khanov for letting him use the cluster facility. S.K.R. is supported in part by the US Department of Energy, Grant Number DE-FG02-04ER41306.

[1] N. Arkani-Hamed, A. G. Cohen and H. Georgi, Phys. Lett. B **513**, 232 (2001);

For reviews, see, for example,

- M. Schmaltz and D. Tucker-Smith, *Ann. Rev. Nucl. Part. Sci.* **55**,229 (2005);
M. Perelstein, *Prog. Part. Nucl. Phys.* **58**, 247 (2007), and references therein.
- [2] C. Csaki, J. Hubisz, G. D. Kribs, P. Meade and J. Terning, *Phys. Rev. D* **67**, 115002 (2003);
J. L. Hewett, F. J. Petriello and T. G. Rizzo, *JHEP* **0310**, 062 (2003);
C. Csaki, J. Hubisz, G. D. Kribs, P. Meade and J. Terning, *Phys. Rev. D* **68**, 035009 (2003);
M. C. Chen and S. Dawson, *Phys. Rev. D* **70**, 015003 (2004);
W. Kilian and J. Reuter, *Phys. Rev. D* **70**, 015004 (2004);
Z. Han and W. Skiba, *Phys. Rev. D* **71**, 075009 (2005).
- [3] I. Low, *JHEP* **0410**, 067 (2004).
- [4] J. Hubisz and P. Meade, *Phys. Rev. D* **71**, 035016 (2005).
- [5] J. Hubisz, P. Meade, A. Noble and M. Perelstein, *JHEP* **0601**, 135 (2006).
- [6] H. C. Cheng and I. Low, *JHEP* **0309**, 051 (2003); *JHEP* **0408**, 061 (2004).
- [7] A. Freitas and D. Wyler, *JHEP* **0611**, 061 (2006).
- [8] A. Belyaev, C. R. Chen, K. Tobe and C. P. Yuan, *Phys. Rev. D* **74**, 115020 (2006).
- [9] M. S. Carena, J. Hubisz, M. Perelstein and P. Verdier, *Phys. Rev. D* **75**, 091701 (2007).
- [10] C. S. Chen, K. Cheung and T. C. Yuan, *Phys. Lett. B* **644**, 158 (2007).
- [11] D. Choudhury and D. K. Ghosh, *JHEP* **0708**, 084 (2007).
- [12] G. Cacciapaglia, S. R. Choudhury, A. Deandrea, N. Gaur and M. Klasen, *JHEP* **1003**, 059 (2010).
- [13] G. Cacciapaglia, A. Deandrea, S. R. Choudhury and N. Gaur, *Phys. Rev. D* **81**, 075005 (2010).
- [14] M. Asano, S. Matsumoto, N. Okada and Y. Okada, arXiv:hep-ph/0602157;
A. Birkedal, A. Noble, M. Perelstein and A. Spray, *Phys. Rev. D* **74**, 035002 (2006).
- [15] B. Bhattacharjee, A. Kundu, S. K. Rai and S. Raychaudhuri, *Phys. Rev. D* **81**, 035021 (2010).
- [16] B. L. Combridge, *Nucl. Phys. B* **151** (1979) 429.
- [17] N. Arkani-Hamed, S. Dimopoulos, G. F. Giudice and A. Romanino, *Nucl. Phys. B* **709**, 3 (2005) [arXiv:hep-ph/0409232];
D. Choudhury, S. K. Gupta and B. Mukhopadhyaya, *Phys. Rev. D* **78**, 015023 (2008) [arXiv:0804.3560 [hep-ph]];
S. Bressler [ATLAS Collaboration and CMS Collaboration], arXiv:0710.2111 [hep-ex].

- [18] M. Perelstein and J. Shao, Phys. Lett. B **704**, 510 (2011) [arXiv:1103.3014 [hep-ph]].
- [19] J. Pumplin, A. Belyaev, J. Huston, D. Stump and W. K. Tung, JHEP **0602**, 032 (2006) [arXiv:hep-ph/0512167].
- [20] M. Cacciari, S. Frixione, M. L. Mangano, P. Nason and G. Ridolfi, JHEP **0809**, 127 (2008) [arXiv:0804.2800 [hep-ph]];
See also, S. Moch and P. Uwer, Phys. Rev. D **78**, 034003 (2008) [arXiv:0804.1476 [hep-ph]];
 N. Kidonakis and R. Vogt, Phys. Rev. D **78**, 074005 (2008) [arXiv:0805.3844 [hep-ph]].
- [21] L. A. Anchordoqui et al., Phys. Rev. Lett. **101**, 241803 (2008).
- [22] S. Cullen, M. Perelstein and M. E. Peskin, Phys. Rev. D **62**,055012 (2000).
- [23] J. L. Hewett and T.G. Rizzo, Phys. Rept. **183**,193 (1989).
- [24] U. Baur,I. Hinchliffe and D. Zeppenfeld, Int. J. Mod. Phys. A **2**, 1285 (1987).
- [25] U. Baur, M. Spira and P. M. Zerwas, Phys. Rev. D **42**,815 (1990).
- [26] P. H. Frampton and S. L. Glashow, Phys. Lett. B **190**,157 (1987)
- [27] E. H. Simmons, Phys. Rev. D **55**, 1678 (1997).
- [28] L. Randall and R. Sundrum, Phys. Rev. Lett. **83**, 4690 (1999).
- [29] T. Sjostrand, S. Mrenna and P. Z. Skands, JHEP **0605**, 026 (2006) [arXiv:hep-ph/0603175].
- [30] M. L. Mangano, M. Moretti, F. Piccinini, R. Pittau and A. D. Polosa, JHEP **0307**, 001 (2003)
- [31] A. Pukhov, arXiv:hep-ph/0412191.
- [32] L. Randall and D. Tucker-Smith, Phys. Rev. Lett. **101**, 221803 (2008)
- [33] P. Schieferdcker et al., CMS Analysis Note-2008/001 (2008);
 CMS Collaboration, *CMS HCAL Technical Design Report*, CERN/LHCC 97-31 (1997).
- [34] ATLAS Collaboration, Report numbes : ATLAS-CONF-2011-102; ATLAS-CONF-2011-089;
- [35] CMS Collaboration, Report Number: CMS-PAS-BTV-11-001.
- [36] [ATLAS Collaboration], arXiv:1112.3832 [hep-ex].
- [37] G. Aad *et al.* [ATLAS Collaboration], arXiv:1109.6572 [hep-ex].
- [38] S. Chatrchyan *et al.* [CMS Collaboration], Phys. Rev. Lett. **107**, 221804 (2011) [arXiv:1109.2352 [hep-ex]].
- [39] S. Chatrchyan *et al.* [CMS Collaboration], JHEP **1108**, 155 (2011) [arXiv:1106.4503 [hep-ex]].
- [40] S. Chatrchyan *et al.* [CMS Collaboration], JHEP **1107**, 113 (2011) [arXiv:1106.3272 [hep-ex]].